Low-spin excitations in ^{95}Zr

T. Rząca-Urban,[1] W. Urban,[1] A. Blanc,[2] M. Jentschel,[2] P. Mutti,[2] U. Köster,[2] G. de France,[3] G. S. Simpson,[4] and C. A. Ur[5]

[1]*Faculty of Physics, University of Warsaw, ul. Pasteura 5, 02-093 Warszawa, Poland*
[2]*Institut Laue-Langevin, 38042 Grenoble, France*
[3]*Grand Accélérateur National d'Ions Lourds (GANIL), CEA/DSM - CNRS/IN2P3, Boulevard Henri Becquerel, BP 55027, 14076 Caen Cedex 5, France*
[4]*LPSC, Université Grenoble-Alpes, CNRS/IN2P3, Institut National Polytechnique de Grenoble, 38026 Grenoble Cedex, France*
[5]*Extreme Light Infrastructure-Nuclear Physics (ELI-NP)/IFIN-HH, 077125 Bucharest-Magurele, Romania*

(Received 7 May 2023; accepted 13 July 2023; published 25 July 2023)

The low-spin structure of the ^{95}Zr nucleus was investigated at Institut Laue-Langevin (Grenoble) by employing three complementary methods: Either cold-neutron capture on ^{94}Zr or cold-neutron-induced fission of ^{235}U, both using the highly efficient EXILL array of high-purity germanium (HPGe) detectors, or β decay of mass-separated ^{95}Y ions at the focal point of the Lohengrin fission-fragment separator. Together 21 new levels and 44 new transitions were placed in the level scheme. Spin-parity assignments to most of the levels in ^{95}Zr were significantly improved.

DOI: 10.1103/PhysRevC.108.014324

I. INTRODUCTION

The odd-A, ^{91}Zr–^{97}Zr isotopes are a source of crucial experimental data on neutron single-particle (s.p.) levels above the $N = 50$ closed shell. The region attracts a lot of attention because of the pronounced phase coexistence effects [1]. The nuclear deformation emerges here due to (among others) the population of $g_{7/2}$ and $h_{11/2}$ neutron shells [2–4], of which especially the latter is poorly evidenced in the $50 \leqslant N \leqslant 60$ range. It is important to learn more about the population of both shells in the region, as well as about the deformation-inducing $9/2^+[404]$ neutron extruder [5], proposed recently in ^{97}Zr [6]. These Zr isotopes are also relevant for studying processes of nucleosynthesis. The $^{95}_{40}$Zr$_{55}$ nucleus is a branching point in the astrophysical s process [7–9]. It is important to know the underlying s.p. structure of Zr isotopes and other properties, such as precise values of neutron-binding energies.

Low-spin states in ^{95}Zr were investigated previously in β decay [10,11], in transfer reactions [8,12,13], and in the thermal-neutron capture reaction ^{94}Zr$(n,\gamma)^{95}$Zr [14]. Only four γ lines were tentatively assigned to ^{95}Zr following the neutron-capture work. High-spin states of ^{95}Zr were studied in fusion-fission experiments [15–17].

Neutron capture may populate levels, especially of a collective nature, which are not populated in other reactions. This makes the neutron-capture measurements, often considered to be a "complete spectroscopy" tool for low-spin excitations, a valuable means to complement other studies. The present work amends previous results with the information from the cold-neutron capture.

In addition to the neutron capture measurement, we revised previous results from β^- decay of the $1/2^-$ ground state of ^{95}Y. Special attention was devoted to spin-parity assignments in ^{95}Zr. In the present work ^{95}Y was produced in thermal-neutron induced fission of ^{235}U and mass $A = 95$ isobars were separated using the Lohengrin fission-fragment separator of Institut Laue-Langevin (ILL) [18]. Another purpose of this measurement was to look for possible isomeric states in ^{95}Zr in a range from nano- to milliseconds. The present work on ^{95}Zr is a continuation of our study of odd-A Zr isotopes [6].

In Sec. II we describe experimental setups and data analysis techniques. In Sec. III the experimental data obtained for the ^{95}Zr nucleus are shown and discussed. Conclusions are presented in Sec. IV.

II. MEASUREMENTS

New levels and transitions in ^{95}Zr were searched for using the data from the neutron-capture reaction on ^{94}Zr, measured with the EXILL detector array and the β decay of ^{95}Y measured with Lohengrin. The progress, compared to previous studies, was possible due to the use in the present work of the very efficient Ge detector arrays at the cold-neutron facility PF1b and at the Lohengrin fission-fragment separator of the Institut Laue-Langevin (ILL) in Grenoble. The use of both data sets helped to eliminate accidental coincidences with lines belonging to contaminating isotopes.

We also used data from the cold-neutron-induced fission of ^{235}U measured with EXILL [19]. The high cumulative yield of ^{95}Y in this reaction provided high-statistics angular correlation data for $\gamma\gamma$ cascades in ^{95}Zr following β decay of ^{95}Y. Triple-γ histograms were used to verify whether such cascades are clean enough to analyze these correlations. Prompt γ rays from ^{95}Zr, produced weakly in ^{235}U $+n$ fission, allowed us to verify properties of levels in the ground-state cascade in ^{95}Zr.

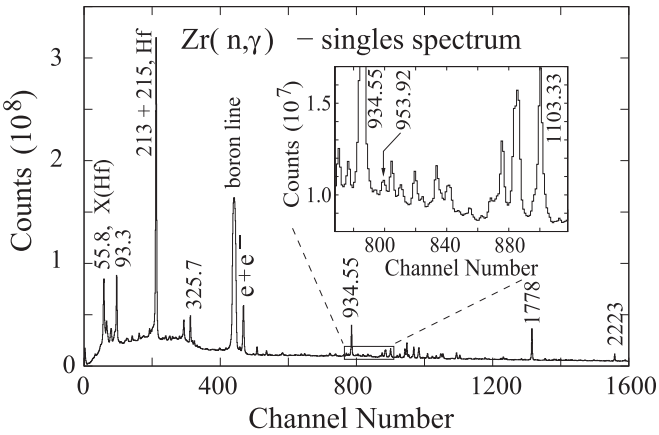

FIG. 1. Low-energy part of the singles γ spectrum from the Zr(n, γ) reaction, measured in this work. Lines are labeled with their γ energies. See text for more comments.

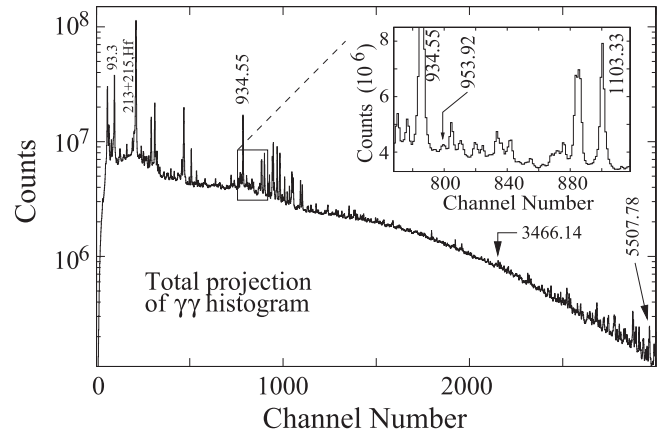

FIG. 2. Total projection of the histogram of $\gamma\gamma$ coincidences from the Zr(n, γ) reaction, measured in this work. Lines are labeled with their γ energies in keV.

A. Cold-neutron capture on ^{94}Zr

The measurement was performed at the PF1b cold-neutron beam of ILL using the EXILL spectrometer consisting of 16 large, high-purity Ge detectors. A detailed description of the experimental facility, the neutron beam collimation system and the target chamber is given in Ref. [19]. The description of the measurement and calibrations is given in our work on ^{97}Zr [6].

The 700 mg target of ZrO_2 used in the measurement contained 19.3% of ^{90}Zr, 5.13% of ^{91}Zr, 7.8% of ^{92}Zr, 8.2% of ^{94}Zr, and 59.6% of ^{96}Zr. The target contained also about of 0.3% of hafnium contamination, which has a neutron-absorption cross section 600 times higher than zirconium. This background contribution was eliminated during the data analysis utilizing the well-known schemes of Hf isotopes populated in (n, γ) reactions.

Figure 1 shows a singles γ spectrum from the cold-neutron capture on the Zr target, as measured in this work, constructed out of 3.3×10^{10} triggerless events collected over 21 h. The spectrum is dominated by γ lines of ^{178}Hf and ^{180}Hf (from Hf contaminations), the 934.55-keV line of ^{92}Zr, a strong line due to the (n, $\alpha\gamma$) reaction on traces of ^{10}B isotope (a probable contamination in the ZrO_2 material) and lines of H_2 (2223 keV) and ^{28}Al (1778 keV) from the capture on the surrounding materials of neutrons scattered on the target (the ^{28}Al lines with very precise energies were used for internal energy calibration [6]). The inset shows the strongest line of ^{95}Zr, corresponding to the 953.92-keV, ground-state transition. The intensity corresponding to ^{95}Zr is estimated to be less than 0.1% of the total intensity collected in the measurement.

To extract from this complex data information on ^{95}Zr we used various two- and three-dimensional (2D and 3D) histograms sorted out of multiple-γ coincidences, created from the triggerless events by applying a 200 ns time window.

Figure 2 displays the total projection of the conventional $\gamma\gamma$ histogram in a range up to 5.6 MeV. Comparing Figs. 1 and 2, one sees that the coincidence requirement removed strong singles contaminating lines (boron, 1778, 2223) and reduced the Compton background, though the coincidences due to Hf isotopes still dominate the spectrum. However, gating on the 953.92-keV line of ^{95}Zr (seen as a weak peak in the inset of Fig. 2), reveals many lines corresponding to transitions in ^{95}Zr, as shown in Fig. 3. Because the 954-keV gate is contaminated by lines belonging to Hf isotopes, there are still contaminating Hf lines seen in the spectrum.

In order to identify uniquely lines of ^{95}Zr, we used histograms with other coincidence conditions. A conventional triple-γ histogram was of help, but particularly useful was the 3D histogram, called ggS3, into which triple-γ events were sorted as follows: Along the S3 axis we sorted the sum of the three γ energies in the event, then out of this triple event three double-γ events were extracted. Out of each of these three double-γ events one γ was sorted along one g axis and the other γ was sorted along the other g axis. The energy difference between the cold neutron capture state and the ground state is a well defined, characteristic signature of each nucleus. Therefore, the gate on the 6462-keV line, corresponding to the neutron binding energy in ^{95}Zr, set on the S3 axis produced clean spectra containing lines in double cascades belonging to ^{95}Zr.

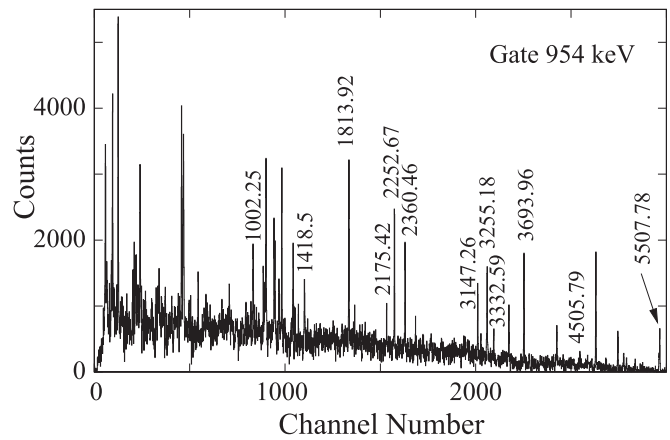

FIG. 3. A γ spectrum gated on the 954-keV line of ^{95}Zr in the $\gamma\gamma$ histogram of coincidences from the Zr(n, γ) reaction, measured in this work. Lines of ^{95}Zr are labeled with their γ energies in keV.

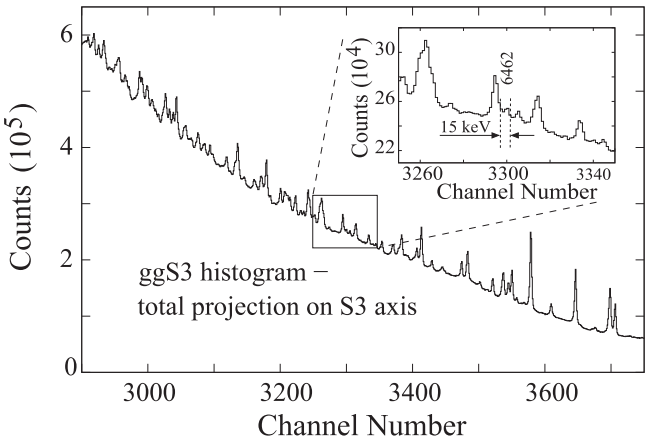

FIG. 4. High-energy part of the spectrum of summed energies of γ rays in threefold cascades following the Zr+n reaction: Total projection on the S3 axis of the ggS3 cube. Lines are labeled with their γ energies. See text for more comments.

Figure 4 displays the high-energy part of the total projection of the ggS3 matrix onto the S3 axis. In the inset the gate on the 6462-keV line is marked. At this high energy the full energy width of the line and the corresponding gate was about 15 keV.

Figure 5 shows a γ spectrum doubly gated on the 6462- and 954-keV lines. The spectrum contains pairs of γ lines with energies summing to 5508 keV (= 6462 − 954 keV), revealing several double-γ cascades linking the neutron capture level with the 954-keV level. One notes a low background level in the spectrum. This is due to the elimination of the usual Compton background by gating on the 6462-keV, energy-sum line.

B. β-decay measurement with Lohengrin

To complement and counter check the (n, γ) data and to search for possible isomeric levels in ^{95}Zr we performed a measurement with the Lohengrin fission-fragment

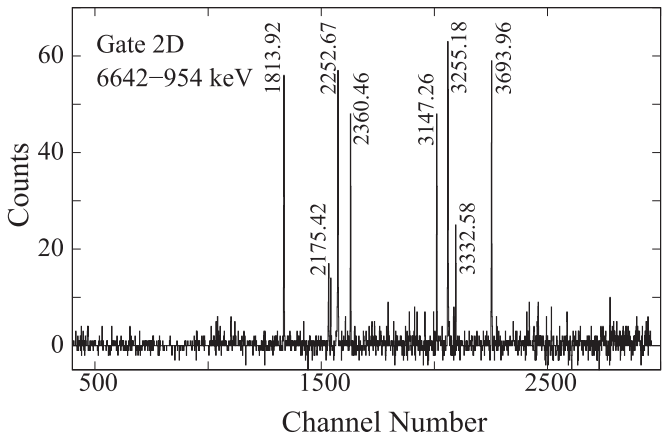

FIG. 5. A γ spectrum doubly gated on the 6642- and 954-keV lines in the ggS3 cube, showing γ rays in twofold cascades depopulating the capture state in the ^{95}Zr nucleus, following the ^{94}Zr +n reaction. Lines are labeled with their γ energies.

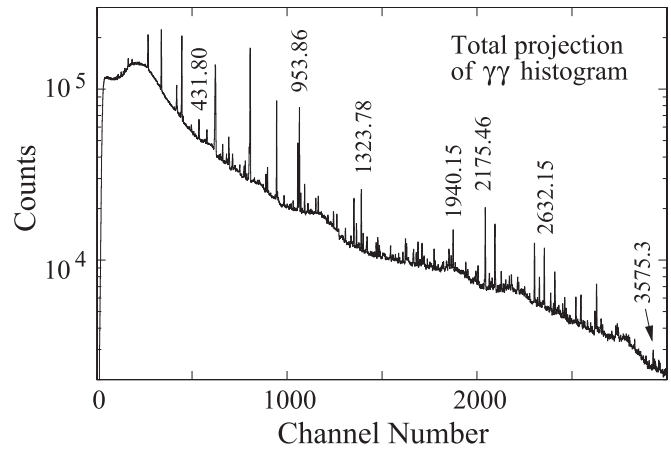

FIG. 6. Total projection of the histogram of $\gamma\gamma$ coincidences from β^- decay of $A = 95$ isobars, collected with Lohengrin. Major lines of ^{95}Zr are labeled with their γ energies in keV.

separator of ILL Grenoble. The measurement provided good γ-coincidence data for verifying and extending the existing information on β decay of ^{95}Y.

Mass $A = 95$ ions from fission of ^{235}U induced by thermal neutrons captured in the Lohengrin beam tube of the ILL reactor were arriving at the detection point about 1.7 μs after being produced. The measurement setup consisted of an ionization chamber and three large Ge detectors placed close to it. The detectors measured γ rays following β^- decays of the ions deposited in an ionization chamber, which registered the time of their arrival.

In the measurement we used an electrostatic deflection system of Lohengrin, operating at a frequency of 100 Hz. The ions collected at the detection point were not transported away. The precise time signals from the ionization chamber and Ge detectors, the chopped beam, and the use of digital electronics with a 40 MHz clock provided the possibility of measuring half-lives in a range from nano- to milliseconds. For more details about such measurements see Refs. [6,20,21].

The 7.5 × 10^6 ions collected in the ionization chamber produced about 4.0 × 10^8 triggerless events, comprising signals from the chamber and Ge detectors. The events were then converted into multiple-γ coincidences using various time windows (from 200 to 600 ns) as well as γ-time events (with the time range from ns to ms), and were sorted into various 2D and 3D histograms.

The quality of the γ-coincidence data is illustrated in Figs. 6 and 7. Figure 6 displays, on a logarithmic scale, the total projection of the γ-γ histogram sorted out of the coincidence events created using a 600-ns time window. The strongest lines of ^{95}Zr reported previously [10,11] are clearly seen in the spectrum. Figure 7 shows a γ spectrum gated in this histogram on the 954-keV line of ^{95}Zr. Again, most of the lines reported in Refs. [10,11] are seen in the spectrum.

The analysis techniques used in this work for time measurements in $A = 95$ isobars were described in Ref. [21]. The high sensitivity of the technique is illustrated in Fig. 11 there, showing a time-delayed spectrum for the 113.8-keV transition from a microsecond isomer in ^{95}Kr, a nucleus produced in

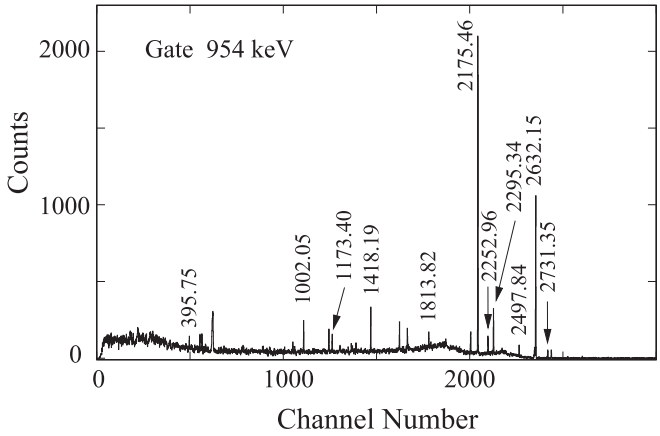

FIG. 7. A γ spectrum gated on the 954-keV line of ^{95}Zr in the $\gamma\gamma$ histogram of coincidences from β^- decay of $A = 95$ isobars, collected with Lohengrin. Lines of ^{95}Zr are labeled with their γ energies in keV.

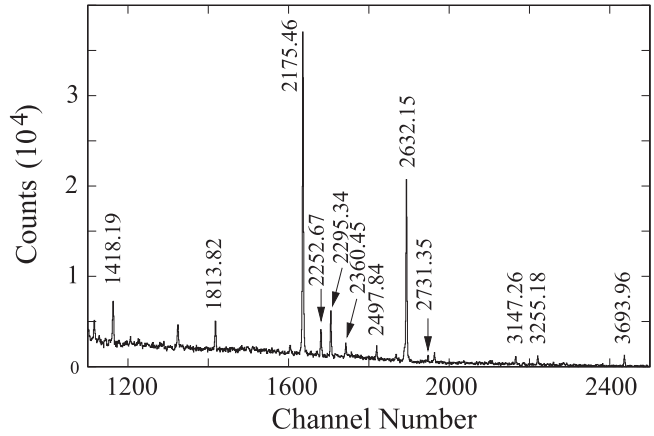

FIG. 8. Part of a γ spectrum gated on the 954-keV line of ^{95}Zr in the $\gamma\gamma$ histogram sorted for angular correlations at 45° out of data collected with EXILL. Lines of ^{95}Zr are labeled with their γ energies in keV. See text for more comments.

fission three times weaker than that of ^{95}Zr. The analysis redone in the present work yields a half-life for this isomer of 1.52(6) μs in good agreement with the precise value of 1.582(22) μs reported recently [22]. The search performed in the present work did not reveal any isomeric states in ^{95}Zr in the 10 ns $< T_{1/2} <$ 10 ms range.

C. Angular correlations with EXILL

To determine angular correlations in ^{95}Zr we used the high-statistics, γ-coincidence data from the EXILL measurement of the cold-neutron-induced fission of ^{235}U [19]. In the data there is a high amount of events corresponding to both, β^- decay of ^{95}Y, produced strongly following fission of ^{235}U as well as due to neutron capture of the natural zirconium, of which an "envelope" around the ^{235}U target was made to stop fission fragments [19].

The 28 Ge-Ge pairs of the eight clover Ge detectors of EXILL, mounted in one plane in octagonal geometry, provided three well defined angles of 0°, 45°, 90° between detectors, used for angular correlations. The description and examples of our angular correlation analysis of the EXILL data can be found in Refs. [19,23].

Figure 8 shows, as an example, a γ coincidence spectrum gated on the 954-keV line in the $\gamma\gamma$ histogram for angular correlations at 45°. One notes that the statistics in the spectrum is about an order of magnitude higher than in the analogous gates shown in Figs. 3 and 7. Thus, although more complex than the clean β-decay data from Lohengrin, the EXILL data may provide better angular correlation results. In the Lohengrin setup there were only two angles (≈0° and ≈90°) with large acceptance because of the close geometry of Ge detectors, maximizing the detection efficiency at the expense of angular resolution.

III. EXPERIMENTAL RESULTS

A. ^{94}Zr (n, γ) reaction

In the thermal neutron capture studies performed so far [14] no primary γ rays were observed and only four weak γ rays of energy 1619.0(3), 2254.1(5), 2994.0(6), and 3117.4(4) keV were tentatively assigned to ^{95}Zr. On the other hand, many low-spin states were reported in β-decay and transfer-reaction works [10–13].

To search for γ transitions in ^{95}Zr, populated in the (n, γ) reaction, we used known lines in ^{95}Zr reported in β decay to construct gated spectra. A careful analysis of the (n, γ) data, using various coincidence histograms described above, allowed us to identify in ^{95}Zr 12 primary γ transitions depopulating the capture state and 20 other transitions connecting low-spin states. These transitions are observed for the first time in (n, γ) cold-neutron capture except, perhaps, the 1618.01- and 2252.67-keV γ lines, which are similar to the 1619.0- and 2254.1-keV lines reported in Ref. [14]. The 2994.0- and 3117.4-keV lines reported there are not seen in the present work.

The level scheme of ^{95}Zr obtained in the present study of the (n, γ) reactions is drawn in Fig. 9 and the properties of levels and their γ decays are listed in Table I. The fourth column (Branch) shows branchings for a level obtained from coincidence spectra gated on a transition feeding this level and normalized to 100 for the strongest branch. In particular, branching values for the neutron-capture level were estimated by comparing counts in $\gamma\gamma$ cascades linking the neutron-capture level and the ground state, because the number of counts in such a cascade depends on the intensity of the primary transition only (this number has to be corrected for the detection efficiency of *both* transitions in a cascade, and the relevant branching ratio of the intermediate level).

Combining branchings from Table I with γ intensities observed in $\gamma\gamma$ coincidence spectra, we estimated relative γ intensities for transitions in ^{95}Zr, as listed in Table II. Because of the complexity of the singles spectrum, seen in Fig. 1, for certain transitions feeding the ground state it was only possible to estimate lower limits of relative γ intensities.

The advantage of the (n, γ) reaction with cold neutrons is that it populates a state situated some milli-electronvolts off

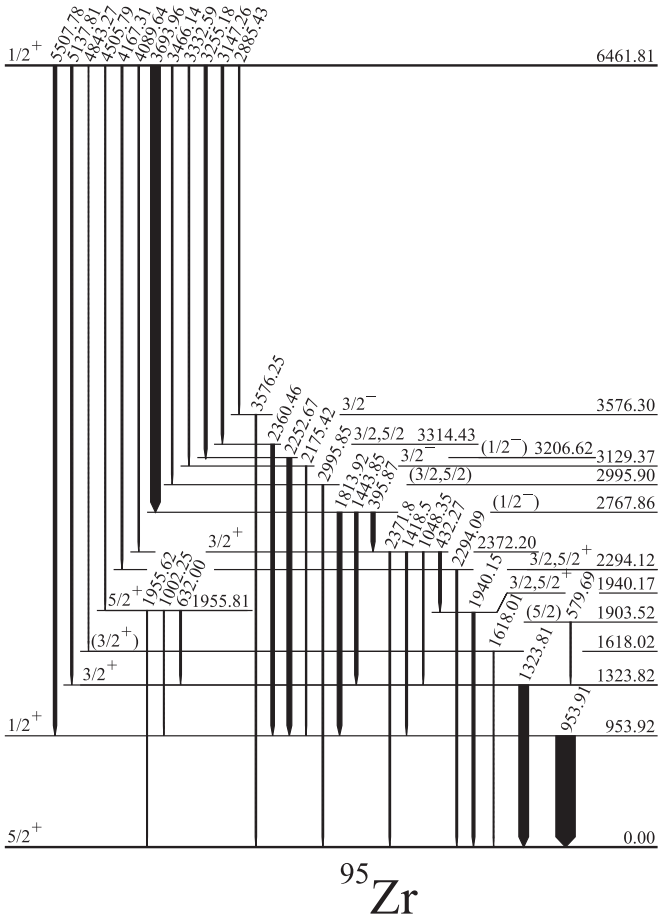

FIG. 9. Partial level scheme of ^{95}Zr obtained in the present work from ^{94}Zr(n,γ) data. The widths of the arrows are proportional to the γ intensity.

the neutron separation energy, only. Therefore such a (n,γ) reaction is a way to determine very precisely the neutron binding energy in a final nucleus, and measurements of γ rays from neutron-capture reactions using arrays of Ge detectors proved to be a good technique for obtaining precise neutron binding energies [6,24]. In Ref. [6] we have shown that the present (n,γ) data may provide precision better than 0.1 keV (see Table VII there).

To find the neutron binding energy of the ^{95}Zr nuclide we analyzed the γ-γ cascades connecting the capture state with the ground state. The relevant energies are given in Table III. The first column shows the energy of the primary transition, obtained from the corresponding E_γ value shown in Table I by correcting for the nuclear recoil. The second column shows the energy of the excited level populated by the transition shown in the first column, taken from Table I. The sum of the two corresponding values is shown in the third column. The weighted average of all summed energies, corresponding to the neutron binding energy S_n of ^{95}Zr, yields $S_n = 6461.81(8)$ keV. This value agrees with the value of 6461.9(9) reported in the compilation [25] and is an order of magnitude more precise. The present uncertainty is a sum of a 0.05 keV statistical uncertainty and the 0.03 keV uncertainty of the energy calibration of EXILL [19].

TABLE I. Properties of levels and transitions in ^{95}Zr obtained in the present work following the ^{94}Zr(n,γ) cold-neutron capture measurement.

E_i (keV)	J_i^π	E_γ (keV)	Branch	E_f (keV)	J_f^π
953.92(5)	$1/2^+$	953.91(5)		0.00	$5/2^+$
1323.82(7)	$3/2^+$	1323.81(7)		0.00	$(3/2^+)$
1618.02(23)	$(3/2^+)$	1618.01(23)		0.00	$5/2^+$
1903.52(16)	(5/2)	579.69(15)		1323.82	$(3/2^+)$
1940.17(9)	$3/2,5/2^+$	1940.15(9)		0.00	$5/2^+$
1955.81(12)	$5/2^+$	632.00(15)	100(12)	1323.82	$(3/2^+)$
		1002.25(20)	81(12)	953.92	$1/2^+$
		1955.62(12)	90(11)	0.00	$5/2^+$
2294.12(11)	$3/2,5/2^+$	2294.09(11)		0.00	$5/2^+$
2372.20(9)	$3/2^+$	432.27(9)	100(6)	1940.17	$5/2^{(+)}$
		1048.35(11)	48(7)	1323.82	$(3/2^+)$
		1418.5(3)	72(9)	953.92	$1/2^+$
		2371.8(3)	59(6)	0.00	$5/2^+$
2767.86(8)	$(1/2^-)$	395.87(8)	88(4)	2372.20	$(3/2^+)$
		1443.85(9)	71(5)	1323.82	$(3/2^+)$
		1813.92(9)	100(6)	953.92	$1/2^+$
2995.90(22)	(3/2,5/2)	2995.85(22)		0.00	$5/2^+$
3129.37(16)	$3/2^-$	2175.42(15)		953.92	$1/2^+$
3206.62(13)	$(1/2^-)$	2252.67(12)		953.92	$1/2^+$
3314.43(15)	3/2,5/2	2360.46(14)		953.92	$1/2^+$
3576.30(15)	$3/2^-$	3576.25(15)		0.00	$5/2^+$
6461.81(8)	$1/2^+$	2885.43(17)	13(2)	3576.10	
		3147.26(13)	23(2)	3314.43	
		3255.18(12)	29(3)	3206.62	
		3332.59(21)	14(3)	3129.37	
		3466.14(22)	15(2)	2995.90	
		3693.96(10)	100(7)	2767.86	
		4089.64(15)	15(3)	2372.20	
		4167.31(14)	17(2)	2294.12	
		4505.79(15)	10(2)	1955.81	
		4843.27(25)	7(2)	1618.02	$(3/2)^+$
		5137.81(13)	22(2)	1323.82	$(3/2^+)$
		5507.78(12)	34(3)	953.92	$1/2^+$

B. β^- decay of ^{95}Y

Table IV lists properties of levels and their decays obtained in the present work in a measurement of β^- decay of ^{95}Y with Lohengrin. The results of the (n,γ) measurement helped to find a number of transitions and levels newly observed in β^- decay, which are marked with an asterisk.

We confirm most of the levels and transitions reported in the compilation [13] except the 2253.6-, 3887.0-, 3926.1-, and 4070.4-keV levels and their decays. The 2253.6-keV decay of the 2253.6-keV level reported in [13] has in our scheme an energy of 2252.96 keV and decays from the new 3206.86-keV level. The 555.5- and 3684.9-keV decays of the 3684.83-keV level reported in [13] are not seen in our data. The compilation [13] places the 1683.0-keV decay in two places of the decay scheme. Our data confirm this but the two decays have visibly different energies. The present work reports generally improved energies and uncertainties of levels and their decays.

TABLE II. Relative γ intensities, I_γ, for transitions in ^{95}Zr as observed in the ^{94}Zr(n,γ) cold-neutron-capture measurement.

E_γ (keV)	I_γ (rel.)	E_γ (keV)	I_γ (rel.)
395.87(8)	42(4)	2360.46(14)	35(5)
432.27(9)	28(3)	2371.8(3)	17(2)
579.69(15)	13(2)	2885.43(17)	13(2)
632.00(15)	19(3)	2995.85(22)	$\geqslant$15
953.91(5)	$\geqslant$208	3147.26(13)	23(2)
1002.25(20)	15(2)	3255.18(12)	29(3)
1048.35(11)	14(2)	3332.59(21)	14(3)
1323.81(7)	$\geqslant$102	3466.14(22)	15(2)
1418.5(3)	21(3)	3576.25(15)	$\geqslant$ 13
1443.85(9)	34(3)	3693.96(10)	100(7)
1618.01(23)	$\geqslant$ 7	4089.64(15)	15(3)
1813.92(9)	48(4)	4167.31(14)	17(2)
1940.15(9)	$\geqslant$ 28	4505.79(15)	10(2)
1955.62(12)	17(2)	4843.27(25)	7(2)
2175.42(15)	12(2)	5137.81(13)	22(2)
2252.67(12)	50(3)	5507.78(12)	34(3)
2294.09(11)	$\geqslant$ 17		

C. Spin-parity assignments to levels in ^{95}Zr

To determine the spin values of the excited states we have analyzed γ-γ angular correlation measurements, where the coincidence rate of two successive γ transitions is analyzed as a function of the angle between them. The angular correlation function between two consecutive γ transitions in a cascade from a nonoriented state can be expressed as a series of Legendre polynomials P_k:

$$W(\theta) = \sum_k A_k P_k(\cos\theta). \quad (1)$$

where θ is the angle between the emission directions of γ_1 and γ_2 in the cascade. The experimental A_k coefficients, obtained from fitting the formula to the experimental data, are compared to theoretical values of A_k coefficients calculated for

TABLE III. Information on two-γ cascades deexciting the capture state to the ground state in ^{95}Zr, as obtained in the present work.

$E_{\text{trans.}}$ (keV)	$E_{\text{exc.}}$ (keV)	Sum (keV)
5507.95(12)	953.92(5)	6461.87(13)
5137.95(13)	1323.82(7)	6461.77(15)
4843.40(25)	1618.02(23)	6461.42(35)
4505.91(15)	1955.81(16)	6461.72(22)
4167.40(14)	2294.12(11)	6461.52(18)
4089.73(15)	2372.20(9)	6461.93(18)
3694.03(10)	2767.86(8)	6461.89(13)
3466.19(22)	2995.90(22)	6462.09(31)
3332.64(21)	3129.37(16)	6462.01(25)
3255.23(12)	3206.62(13)	6461.85(18)
3147.30(13)	3314.43(15)	6461.73(20)
2885.47(17)	3576.30(15)	6461.77(24)

TABLE IV. Levels and transitions of ^{95}Zr observed in the present work following β^- decay of the $1/2^-$ ground state of ^{95}Y. New data are marked with asterisks.

E_i (keV)	J_i^π	E_γ (keV)	I_γ (rel.)	E_f (keV)
953.87(5)	$1/2^+$	953.86(5)	100(3)	0.00
1323.79(5)	$3/2^+$	1323.78(5)	26(2)	0.00
1618.13(9)	$(3/2^+)$	1618.11(9)	8.1(6)	0.00
1721.51(9)	3/2,5/2	397.74(13)	0.8(3)	1323.79
		1721.50(12)	1.3(3)	0.00
1893.07(7)	$(5/2^+)$	569.30(7)	1.8(2)	1323.79
		939.44(15)*	0.4(2)	953.87
		1892.96(9)	2.4(4)	0.00
1903.85(8)	(5/2)	580.20(9)	1.3(4)	1323.79
		1903.57(17)	1.6(4)	0.00
1940.16(7)	$3/2,5/2^+$	1940.15(7)	15(1)	0.00
1955.98(6)	$5/2^+$	632.31(7)	2.6(3)	1323.79
		1002.05(8)	2.3(2)	953.87
		1955.85(9)	2.8(3)	0.00
2371.98(6)	$3/2^+$	431.80(6)	12(1)	1940.17
		754.37(9)*	2.1(4)	1618.13
		1048.25(7)	5.8(5)	1323.79
		1418.19(8)	3.2(3)	953.87
		2371.91(15)	6.7(5)	953.87
2767.74(6)*	$(1/2^-)$	395.75(8)*	2.2(3)	2372.01
		1443.95(7)*	1.5(3)	953.87
		1813.82(10)*	2.0(2)	953.87
2890.6(5)*		1936.7(5)*	0.6(1)	953.87
3129.38(9)	$3/2^-$	1173.40(15)	6.1(5)	1956.10
		1225.75(25)	1.8(3)	1903.85
		1407.87(12)	2.2(4)	1721.51
		1511.38(9)	4.6(4)	1618.13
		1805.42(9)	7.9(6)	1323.79
		2175.46(8)	45(2)	953.87
3206.86(7)*	$(1/2^-)$	2252.96(5)*	0.4(2)	953.87
3249.22(7)	$1/2^+$,3/2	1293.28(12)	2.0(4)	1956.00
		1309.16(17)	1.5(2)	1940.17
		1356.32(15)	3.2(3)	1893.07
		1527.47(18)	1.3(3)	1721.51
		1631.4(2)	1.3(4)	1618.13
		1925.30(7)	2.8(5)	1323.79
		2295.34(7)	7.7(4)	953.87
3451.50(14)	$(5/2^+)$	1833.52(17)	1.0(2)	1618.13
		2127.54(15)	1.5(4)	1323.79
		2497.84(16)	2.0(4)	953.87
3575.80(11)	$3/2^-$	446.5(2)*	0.7(2)	3129.42
		1635.33(19)	0.9(2)	1940.16
		1682.88(13)	2.0(3)	1893.07
		1854.21(15)	1.4(3)	1721.51
		2251.98(17)	0.4(2)	1323.79
		2621.81(15)	1.4(3)	953.87
		3575.3(4)	43(2)	0.0
3586.18(8)	$(1/2^-)$	456.70(9)*	0.9(3)	3129.42
		1214.22(18)	0.5(2)	2372.01
		1629.85(25)	1.3(3)	1956.00
		1682.30(9)	1.0(2)	1903.85

TABLE IV. (*Continued.*)

E_i (keV)	J_i^π	E_γ (keV)	I_γ (rel.)	E_f (keV)
		1967.85(12)	1.0(2)	1618.13
		2632.15(9)	29(2)	953.87
3685.26(12)		2731.35(11)	1.4(3)	953.87
3714.97(15)*		2761.05(14)*	1.3(3)	953.87
3853.0(3)*		2899.0(3)*	0.8(2)	953.87
3977.6(3)*		3023.6(3)*	0.4(1)	953.87
4450.1(7)*		3496.1(7)*	0.2(1)	953.87

various hypotheses of spins, multipolarities and mixing ratios, to find the solutions.

The cold-neutron capture on the 0^+ ground state of ^{94}Zr produces a capture level in ^{95}Zr with well defined spin-parity $1/2^+$. As the $5/2^+$ spin-parity of the ground state in ^{95}Zr is also known [13], spins of some intermediate levels within $\gamma\gamma$ cascades linking the capture level and the ground state can be determined. The $\gamma\gamma$ cascades linking the capture level and the $1/2^+$ level at 953.92 keV may show large anisotropy in case the intermediate level has spin 5/2. However, cascades with the $1/2^+$, 953.92-keV intermediate level will all be isotropic. Cascades funneling through an intermediate level with spin 3/2 will have the A4 coefficient equal zero.

Table V lists results of angular correlation analyses for $\gamma\gamma$ cascades in ^{95}Zr, as obtained in the present work (we used the more precise γ energies listed in Table IV and if not available, energies from Table I). If mixing ratios δ are not known for both transitions in a cascade some estimates can be made when more cascades involving one of the two transitions are available.

Intensities of primary γ transitions also give some hints on spins of the levels they populate, as discussed in Ref. [6]. Generally, one observes primary γ transitions corresponding to spin change $\Delta I \leqslant 2$, only, and intensities of $\Delta I = 2$ quadrupole transitions, are, usually, several times weaker than intensities of $\Delta I \leqslant 1$ transitions. In the following we combine the present (n, γ) and β-decay data with the data reported in the compilation [13] to propose spins and parities in ^{95}Zr.

953.87-keV level. The 1/2 spin of the 953.87-keV level reported in Ref. [13] is confirmed by angular correlations for five cascades funneling through this level, shown at the top of Table V, which are highly isotropic. The precise results for the 2175.46–953.86-keV and 2632.15–953.86-keV cascades support the correctness of our angular correlation analysis.

1323.79-keV level. Angular correlations of various γ transitions with the 1323.78-keV transition show pronounced anisotropies. Therefore, the spin of the 1323.79-keV level is not 1/2. Furthermore, the correlation in the 5137.81–1323.78-keV cascade is not consistent with spin 5/2 of the 1323.79-keV level, as seen in Fig. 10, where the blue rectangle represents experimental A_2/A_0 and A_4/A_0 values with uncertainties from Table V and the ellipse shows possible solutions for A_2/A_0 and A_4/A_0 pairs in the 1/2–5/2–5/2 cascade as a function of δ mixing ratio, ranging from 0.0 to $\pm\infty$. The 3/2 spin solution for the 1323.79-keV level is supported by small A_4/A_0 values in the four cascades involving the 1323.78-keV transition, as shown in Table V under "gate 1324 keV."

TABLE V. Angular correlation coefficients for γ-γ cascades in ^{95}Zr. See text for more information on the δ mixing ratios.

$E_{\gamma1}$–$E_{\gamma2}$	A_2/A_0	A_4/A_0	$\delta(\gamma_1)$	$\delta(\gamma_2)$
gate 954 keV				
1418.19–953.86	−0.004(57)	0.076(117)		
2175.46–953.86	0.004(10)	−0.005(21)		
2252.96–953.86	−0.042(41)	0.096(88)		
2295.34–953.86	0.042(39)	−0.012(87)		
2632.15–953.86	0.001(11)	0.001(24)		
gate 1324 keV				
1048.25–1323.78	−0.160(30)	−0.095(60)		
1805.42–1323.78	−0.330(25)	0.041(47)	0.01(2)	0.9
1925.30–1323.78	−0.263(61)	−0.015(117)		
5137.81–1323.78	−0.611(70)	0.062(126)	−0.8(2) or −4(2)	0.9(4)
gate 1721 keV				
1407.87–1721.50	−0.43(18)	0.45(34)		
1854.21–1721.50	−0.57(11)	0.30(20)		
gate 1893 keV				
1356.32–1892.96	0.123(57)	0.336(153)	0.00	2.6(7)
1682.88–1892.96	−0.175(98)	0.088(172)	0.01	1.6(9)
gate 3694 keV				
3693.96–395.87	0.025(58)	0.059(124)		
3693.96–1443.95	0.077(92)	−0.133(206)		
3693.96–1813.82	−0.059(58)	−0.101(123)		
other cascades				
1511.38–1618.11	0.090(38)	0.008(81)		
116.5–1676.6	0.239(78)	−0.265(194)		
1682.30–1903.57	0.300(109)	0.128(256)		
431.80–1940.15	−0.146(16)	−0.020(32)		
1173.40–1955.85	0.161(82)	0.07(19)	0.0(9)	−1.2(6)
3147.26–2360.46	0.244(57)	0.094(137)		
3255.18–2252.96	−0.001(41)	−0.146(91)		
3466.14–2995.85	0.11(9)	−0.14(21)		

Using these four cascades we estimated the mixing ratio of the 1323.78-keV transition to be $\delta = 0.9(4)$. The large δ value indicates positive parity for the 1323.79-keV level. With this value one finds the mixing ratio δ of −0.8(2) or −4(2) for the 5137.81-keV transition. The large admixture of an $E2$ multipolarity is consistent with the low intensity of this $\Delta I = 1$ transition.

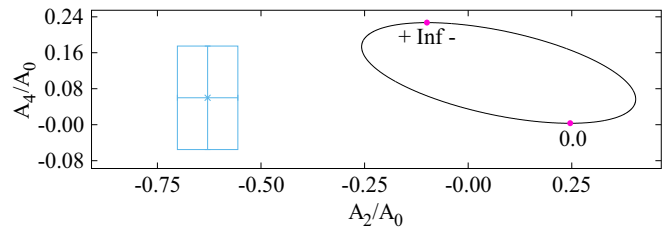

FIG. 10. Angular correlations for the 1/2-5/2-5/2 spin hypothesis in the 5137.81-1323.78-keV cascade in ^{95}Zr, as observed in the present angular correlations from EXILL. In calculating angular correlations the 5137.81-keV transition is assumed to be a stretched quadrupole with $\delta = 0$. See text for more comments.

1618.13-keV level. The nonzero anisotropy of angular correlations for the 1511.38–1618.11-keV cascade indicates spin higher than 1/2 for the 1618.11-keV level. Spin-parity $(3/2)^+$ reported in Ref. [13] is consistent with the primary feeding of this level in the (n,γ) reaction.

1721.51-keV level. No primary γ decay to the 1721.51 level is seen, which supports $(5/2^+)$ spin-parity reported in Ref. [13]. The very anisotropic correlations shown in Table V under "gate 1721 keV" exclude spin 1/2 for the 1721.51-keV level.

1793.1-keV level. An important result of the present work is the verification of the spin-parity assignment to the 1793.1(2)-keV level of the yrast, ground-state cascade in ^{95}Zr. The 1793.1-keV level was tentatively assigned spin-parity $11/2^-$ in Ref. [16] and $9/2^+$ in Ref. [17], based on systematics. In the latter work a 12% decay branch of 1792.6 keV from the level in question to the $5/2^+$ ground state is reported, assumed to be an $E2$ rather than $E3$ transition, thus supporting the $9/2^+$ spin-parity assignment.

The present prompt-γ data from fission of ^{235}U induced by neutrons provided angular correlations for the 116.5(1)–1676.6(1)-keV cascade deexciting the 1793.1-keV level (note some differences in energies relative to Refs. [16,17], where uncertainties were larger). The present results exclude spin-parities $11/2^-$-$9/2^+$-$5/2^+$ (i.e. stretched $E1$–$E2$ transitions) in the cascade, as proposed in Ref. [16]. The 12%, 1792.6-keV decay branch reported in Ref. [17] further indicates that the spin-parity of the 1793.1-keV level is not $11/2^+$ and also not 7/2, leaving spin 9/2 as the most probable solution.

Our angular correlation are consistent with two spin-parity assignments for the discussed cascade, the $9/2^+$-$7/2^+$-$5/2^+$ solution proposed in Ref. [17] with $\delta(116.5)$ in the range from 0.5 to 1.4 and $\delta(1676.6)$ equal 0.6(2) or 3.8(7) (one notes that these δ values exclude the $9/2^-$-$7/2^+$-$5/2^+$ solution) and the other, $9/2^-$-$9/2^+$-$5/2^+$ solution, with $\delta(116.5) = -0.17(30)$.

1893.07-keV level. The compilation [13] reports firm $3/2^+$ spin-parity for this level based on data from a transfer-reaction measurement. However, this assignment is not consistent with other observations. The large A4 coefficient of angular correlations for the 1356.32–1892.96-keV cascade favors spin 5/2 for the 1893.07-keV level, which is supported by the nonpopulation of this level in the (n,γ) data. The 5/2 assignment is also consistent with the weak population in β^- decay, reported in the compilation [13].

The best fit to the experimental correlation is obtained for the 1/2–5/2–5/2 spin hypothesis in the 1356.32–1892.96-keV cascade, giving $\delta(1892.96) = 2.6(8)$. Such a large mixing suggests positive parity for the 1893.07-keV level.

1903.85-keV level. The large anisotropy of the angular correlation for the 1682.30–1903.57-keV cascade excludes spin 1/2 for the 1903.85-keV level. Both 3/2 and 5/2 spins are allowed by correlations. Spin 5/2 is preferred because of no primary γ decay to the 1903.85-keV level.

1940.16-keV level. The spin of the 1940.16-keV level is not 1/2 because of the anisotropic angular correlations in the 431.80–1940.15-keV cascade. The lack of the primary decay from the neutron-capture level suggests spin 5/2 for this level, but spin 3/2 is also consistent with angular correlations.

1955.81-keV level. Spin 5/2 and tentative positive parity are reported for the 1955.98-keV level [13]. Positive parity is supported by angular correlation for the 1173.40–1955.85-keV cascade, calculated for the spin sequence 3/2–5/2–5/2 with a large $\delta(1955.85) = -1.2(6)$.

2294.12-keV level. The 2294.12-keV level is populated moderately following the (n,γ) reaction. This suggests spin 3/2 or 5/2 for the level. Angular correlations for the 4167.31–2294.09-keV cascade are consistent with both solutions. The nonobservation of this level in β decay of ^{95}Y favors spin 5/2. Positive parity for this spin is supported by the primary decay to the 2294.12-keV level.

2371.98-keV level. The present data are consistent with spin-parity $3/2^+$ reported in [13] for the 2371.98-keV level.

2767.86-keV level. The angular correlation for the 3693.96–1813.82-keV cascade is not consistent with spin 5/2 for the 2767.86-keV level because for the 1/2–5/2–1/2 spin sequence (two stretched quadrupole transitions) the expected coefficients are $(A_2/A_0)^{th} = 0.286$ and $(A_4/A_0)^{th} = 0.381$. The 1/2 spin is preferred over the 3/2 solution because of the rather isotropic character of all three cascades going through the 2767.86-keV level and the lack of the decay to the $I = 5/2$ ground state. This absence and the high intensity of the 3693.96-keV, primary transition suggests negative parity for the 2767.86-keV level.

2995.90-keV level. Spins $(3/2, 5/2)$ are tentatively assigned to this level considering the observed population by the 3466.16-keV primary transition. Angular correlations, are rather inconclusive, though consistent with both options. The nonobservation of this level following β decay favors spin 5/2 solution.

3129.38-keV level. Spins 5/2 and 1/2 are not supported by our correlations for the 1805.42–1323.78-keV cascade. This leaves spin 3/2 solution for the 3129.38-keV level. Negative parity is adopted after Ref. [13]. For the 1805.42-keV transition the δ mixing ratio is 0.01 or –3.8, as obtained from angular correlations for the 1805.42–1323.78-keV cascade with $\delta(1323.78) = 0.9$. The 0.01 value is favored due to the $E1$ character of this transition.

3206.62-keV level. For the 1/2–5/2–1/2 spin sequence the calculate coefficients are $(A_2/A_0)^{th} = 0.286$ and $(A_4/A_0)^{th} = 0.381$. This solution is rejected by the experimental angular correlations for the 3255.18–2252.96-keV cascade, which allow spins 1/2 and 3/2, only. Spin-parity $1/2^-$ is favored by the nonobservation of any 3206.57-keV decay to the ground state (its intensity is lower than 1% of the intensity of the 2252.96-keV line).

3249.22-keV level. Spin 5/2 is unlikely considering $\log ft = 5.8$ [13] to this level and the lack of any primary feeding in (n,γ). Spin-parity is $1/2^-$ is not likely because of the strong decay to the $5/2^+$ ground state, but spin $1/2^+$ is possible. Angular correlations for the 1356.32–1892.96-keV and 1925.30–1323.78-keV cascades allow both 1/2 and 3/2 spins.

3314.43-keV level. Angular correlations for the 3147.26–2360.46-keV cascade allow spins 3/2 and 5/2 with the 1/2–3/2–1/2 spins in the cascade fitting better the experimental data.

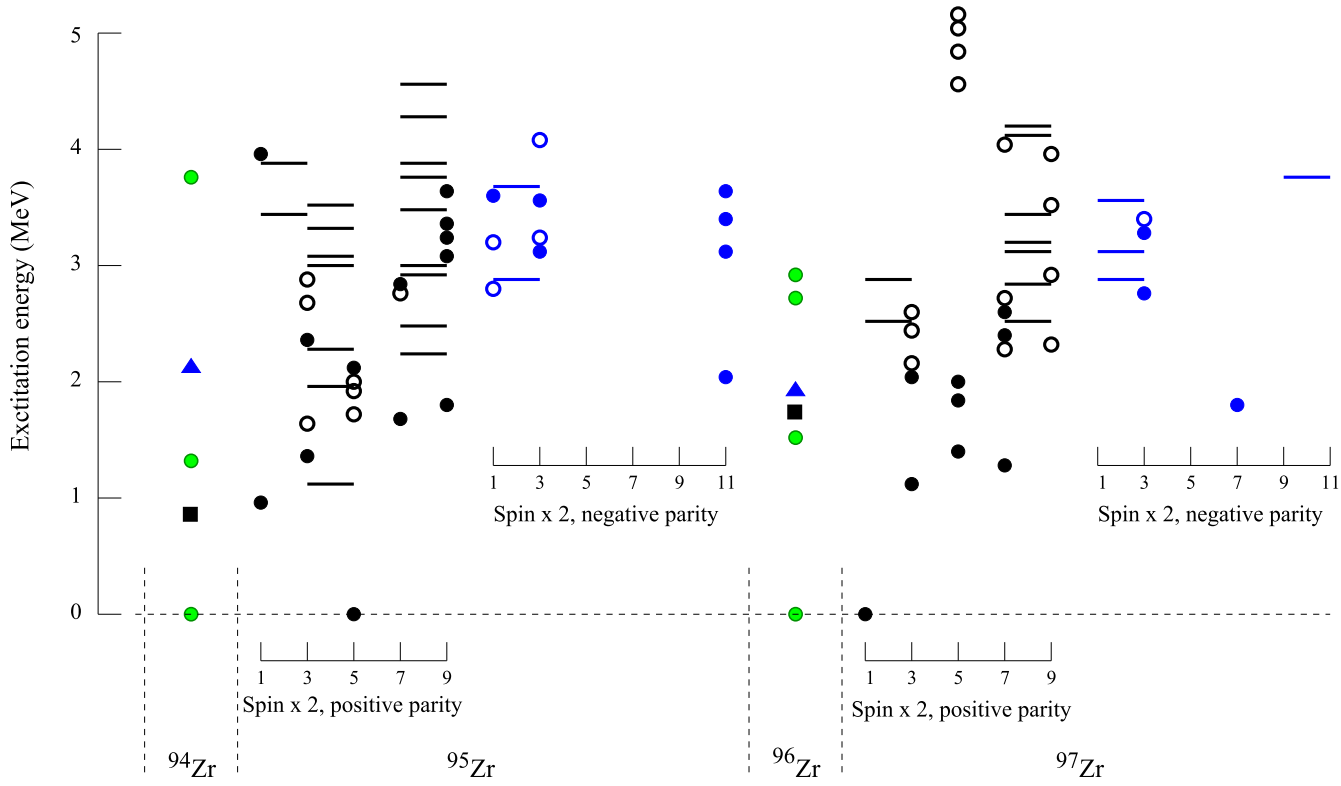

FIG. 11. Low-spin excitations in ^{95}Zr and ^{97}Zr nuclei. See text for the description of symbols used in ^{95}Zr and ^{97}Zr. The 0^+ (circles), 2_1^+ (squares), and 3_1^- (triangles) levels in ^{94}Zr and ^{96}Zr core nuclei are also shown to help the discussion. The data are taken from Refs. [6,13,29] and from the present work.

3451.50-keV level. This level is not seen in our (n,γ) data, which suggests spin 5/2. This is not consistent with the reported log ft value [13]. On the other hand we note that for high-energy levels weakly populated in β decay such log ft values should be rather seen as lower limits.

3575.75-keV level. The log $ft = 4.92$ reported for the 3575.75-keV level indicates negative parity and spin 1/2 or 3/2 for this level. Spin-parity $1/2^-$ is rejected because of the dominating decay branch to the $5/2^+$ ground state, leaving $3/2^-$ spin-parity solution. Angular correlations are consistent with the $3/2^-$-$5/2^+$-$5/2^+$ spin-parity sequence in the 1682.88–1892.96-keV cascade.

3586.20-keV level. The compilation [13] reports spin $1/2^-$ or $3/2^-$ for the 3586.20-keV level. Spin $1/2^-$ is favored because of no decay to $5/2^+$ g.s. Angular correlations for the 1682.30–1903.57-keV cascade give a good fit for 1/2–5/2–5/2 spins in the cascade, with $\delta(1903.57) = 0.16(3)$ or 1.2(6). The 0.16 value is preferred because of the negative parity of the 1903.85-keV level in this case.

One notes that with spin-parity $1/2^-$ the 1629.85-keV decay from the 3586.20-keV level to the $5/2^+$ level at 1955.98 keV should have a $M2$ multipolarity, which is consistent with its low intensity.

IV. DISCUSSION

Reliable s.p. energies are vital for testing model calculations of structure of odd-A nuclides. The mean-field calculations of Zr isotopes [26] offer a qualitative insight into the evolution of the structure of odd-A Zr isotopes, showing that the ^{95}Zr nucleus may be the lightest one in the chain where some collective, low-spin excitations occur. However, these calculations do not reproduce the experimental data quantitatively. The (n,γ) data may help improve model calculations by hinting toward levels with a collective nature.

With the $\nu d_{5/2}$ and $\pi p_{1/2}$ closed shells the ^{96}Zr nucleus is a well defined core for both odd-A neighbors. In the $1/2^+$ ground state of ^{97}Zr the odd neutron occupies the $\nu s_{1/2}$ shell and one expects excited levels due to the promotion of the odd neutron to the $\nu g_{7/2}$ and $\nu h_{11/2}$ shells. The ground state of ^{95}Zr is formed by the $\nu d_{5/2}$ hole in the ^{96}Zr core. However, ^{95}Zr can be also seen as an odd neutron coupled to the ^{94}Zr core and one may expect excited levels due to the promotion to the $s_{1/2}$, $g_{7/2}$, and $h_{11/2}$ neutron levels. Furthermore, the odd neutron occupying these shells may couple to the 2_1^+ and 3_1^- excitations of the ^{94}Zr and ^{96}Zr cores. Such coupling will produce excited levels of the (s.p. $\otimes\, 2^+$) and (s.p. $\otimes\, 3^-$) nature and also the so-called anomalous-coupling levels, $(\nu d_{5/2}^n)_{j,j-1}$. One also expects coupling of the available neutron levels to excited 0^+ levels in both cores, a mechanism well documented in Refs. [27,28]. Therefore, many various low-spin levels should appear in ^{95}Zr and ^{97}Zr.

Figure 11 displays about forty low-spin levels in each of the two nuclei, much more than expected in a simple, spherical-core-plus-neutron systems (we note that numerous levels in both ^{95}Zr and ^{97}Zr, reported in Refs. [6,13,29] and in the present work, with no information on spin, are not shown in Fig. 11). Levels with firm spin-parity assignment are

represented by filled symbols, those with tentative assignment are shown as empty symbols, while bars represent levels with j or $j+1$ assignment. The present neutron-capture data limited the spin uncertainties of prior β decay works, where many levels were reported with spins ranging from j to $j+2$ [13]. To help the discussion, basic levels in ^{94}Zr and ^{96}Zr core nuclei are also shown.

In Ref. [6] we discussed the nature of low-spin excitations in ^{97}Zr. Some information about the structure of ^{95}Zr can be obtained by comparing its low-spin levels with low-spin levels in ^{97}Zr.

A. Positive-parity levels in ^{95}Zr and ^{97}Zr

Excited states in ^{97}Zr with spin-parity $7/2^+$, populated in the allowed β^- decay of the $9/2^+$ isomer in ^{97}Y, are not populated in the ^{96}Zr(n,γ) reaction. Such levels are also not populated in ^{95}Zr following the ^{94}Zr(n,γ) reaction and in β^- decay of the $1/2^+$ g.s. of ^{95}Y. However, a number of $7/2^+$ levels in ^{95}Zr were observed in transfer-reaction measurements [13].

The $7/2^+$ levels in ^{97}Zr, shown in Fig. 11, are most likely due to the $g_{7/2}$ neutron level fragmented by the ^{96}Zr core collectivity [6]. The lowest one seen at 1264 keV is clearly identified as the $g_{7/2}$ s.p. neutron [13].

Analogous $7/2^+$ levels in ^{95}Zr are expected at higher energies. The $1/2^+$ level due to the $s_{1/2}$ neutron, forming the ground state in ^{97}Zr, in ^{95}Zr appears at 954 keV. Therefore, the lowest $7/2^+$ level of the $g_{7/2}$ origin is expected in ^{95}Zr about 1 MeV higher than in ^{97}Zr. The 2250 keV level in ^{95}Zr, with $7/2^+$ or $9/2^+$ assignment, is a possible candidate. The $7/2^+$ level at 1676.6 keV in ^{95}Zr, verified in this work is, most likely, a collective excitation due to coupling of the 1750-keV, 2_1^+ excitation in ^{96}Zr to the $d_{5/2}$ neutron hole, which produces also the $9/2^+$ level at 1793.1 keV.

In ^{97}Zr we proposed that the 2264.3 keV level corresponds to the $9/2^+[404]$ extruder of the $\nu g_{9/2}$ origin. One may ask if there are analogous excitations in ^{95}Zr. Figure 11 shows four excitations around 3.2 MeV in ^{95}Zr identified as $9/2^+$ levels [13]. In ^{97}Zr the $\log ft \approx 5.4$ values for $9/2^+$ levels suggest the (retarded) allowed β^- decay transition of $\pi g_{9/2}(\nu g_{9/2}^2)_{0^+} \rightarrow (\pi g_{9/2}^2)_{0^+}\nu g_{9/2}$ nature, supporting their $g_{9/2}$ neutron origin. In ^{95}Zr such data are not available.

We note that there are more levels in ^{95}Zr than in ^{97}Zr, especially those with spin-parity $3/2^+$ and $5/2^+$ states. In fact, up to seven $5/2^+$ states can be produced by coupling the $\nu d_{5/2}$ particle (hole) to 0^+ levels in ^{94}Zr (^{96}Zr) cores. Analogous coupling to $\nu g_{7/2}$ may produce four $7/2^+$ levels in ^{97}Zr.

Any better description of ^{95}Zr and ^{97}Zr, either phenomenological or theoretical, expected to improve the data on s.p. neutron energies in the region [30,31] will require, first of all, better spin-parity assignments to excited levels. A high-statistics (n,γ) experiment with a highly enriched ^{94}Zr target and improved transfer-reaction measurements may serve the purpose.

B. Negative-parity levels in ^{95}Zr and ^{97}Zr

The s.p. energy of the $\nu h_{11/2}$ shell is important for the interpretation of octupole excitations in the $A \approx 100$ region. The calculations imply that there is no stable octupole deformation around $N = 56$ in this region [32], but the softness of the nuclear potential in the β_3 direction suggests octupole vibrations are present, which are indeed strong in ^{96}Zr [33]. Two types of octupole modes were proposed in the region: The common scalar and the higher-energy isovector octupole coupling [31].

To determine the effective $\nu h_{11/2}$ position, energies, and spectroscopic factors for $11/2^-$ excited levels with unique spin-parity identification are needed. The effective energies reported in Refs. [30,31,34] may need verification because of new findings:

(i) In ^{97}Zr the 2264-keV level was interpreted in the past as being due to $\nu h_{11/2}$ s.p. excitation [35], but in Ref. [6] it was assigned spin-parity $9/2^+$. The 3791-keV levels with spin-parity $9/2^-$ or $11/2^-$ [13] may be an octupole phonon coupled to the $5/2^+$ level at 1400.3 keV. Thus, the $\nu h_{11/2}$ s.p. level remains unknown.

(ii) In ^{95}Zr we rejected $11/2^-$ assignment to the 1793-keV level proposed in [16]. The $11/2^-$ level is now placed at 2022 keV, as proposed by Pantelica [17].

(iii) In ^{97}Zr the $7/2^-$ excited level at 1807.5 keV [6] was interpreted as being due to an octupole phonon coupled to the $1/2^+$ ground state [35]. Its energy coincides with the 1897-keV excitation energy of the 3_1^- level in ^{96}Zr [33]. Analogous octupole excitation on top of the ground state in ^{95}Zr may be the $11/2^-$ level at 2022.3-keV [17], considering the 2057.63-keV excitation energy of the 3_1^- level in ^{94}Zr [36].

(iv) In ^{95}Zr there are three more $11/2^-$ levels, shown in Fig. 11. They are located around 3.3 MeV and could correspond to the octupole phonon coupled to $5/2^+$ levels seen around 1.9 MeV. On the other hand the 3731-keV level in ^{97}Zr with $9/2^-$ or $11/2^-$ spin-parity was interpreted as being due to $\nu h_{11/2}$ excitation, though with the spectroscopic factor of 0.13, only [37]. As suggested in Refs. [31,37] the $\nu h_{11/2}$ excitation should show up in ^{95}Zr at lower energy. Therefore, one of the three discussed $11/2^-$ levels in ^{95}Zr may correspond to the $\nu h_{11/2}$ excitation. It is of high interest to verify this suggestion in order to learn more about the enigmatic $\nu h_{11/2}$ level.

There are a number of $1/2^-$ and $3/2^-$ levels around 3 MeV in ^{97}Zr, which are strongly populated in β^- decay of the $1/2^-$ ground state of ^{97}Y [29]. Their $\log ft$ values indicate an allowed transition of a likely $[\pi p_{1/2}(\nu g_{7/2}^2)_{0^+}]_{1/2^-} \rightarrow [\pi p_{1/2}(\nu g_{7/2}\pi g_{9/2})_{1^+}]_{1/2^-,3/2^-}$ nature (the allowed $(\nu g_{7/2}^2)_{0^+} \rightarrow (\nu g_{7/2}\pi g_{9/2})_{1^+}$ decay of even-even cores is common in the region; see Ref. [38] and references therein) and, consequently, a rather s.p. nature of these levels.

In ^{95}Zr, levels with spin-parity $1/2^-$ or $3/2^-$ are seen in a similar excitation energy range as in ^{97}Zr. The $\log ft$ values of these levels are a bit higher than in ^{97}Zr but still indicative of an allowed decay of the $1/2^-$ ground state of ^{95}Y, which points to the same nature of this β^- transition as

in ^{97}Zr. However, in this case one would expect these levels to appear at higher energy than in ^{97}Zr. As this is not the case, their structure may be more complex than suggested above. Detailed shell-model calculations may help to interpret these low-spin levels.

V. SUMMARY

Many new low-spin states in the ^{95}Zr nucleus were observed following the cold-neutron capture on ^{94}Zr or neutron-induced fission of ^{235}U respectively, using the high-efficiency Ge detector array EXILL at ILL Grenoble. The neutron binding energy and excitation energies of other excited levels were determined more accurately. The previously reported results from β^- decay of ^{95}Y were also verified using the Lohengrin fission-fragment separator of ILL. Spin-parity assignments to levels of ^{95}Zr were improved using precise angular correlations measured with EXILL.

Of many low-spin levels of various natures expected in ^{95}Zr, those with dominating s.p. nature dominate, though the present (n, γ) data have revealed three levels not populated in β^- decay, thus of probable collective nature. No evidence for s.p. levels originating from either $h_{11/2}$ or $g_{9/2}$ neutron shells was obtained to date. It is likely that the $9/2^+[404]$ orbital, observed in ^{97}Zr, ^{99}Zr and ^{101}Zr isotopes is not formed in ^{95}Zr because of the spherical shape of this nucleus. The $\nu h_{11/2}$ level remains largely unknown in the region and the present work points to the need of verifying its effective s.p. energy, because some of the levels reported previously with spin-parity $11/2^-$ were shown to have different spins. The common presence of octupole excitations, reported previously, also needs verification.

The present work has shown how much is still unknown about excitations in the spherical, odd-A Zr isotopes. More than half of low-energy, low-spin levels in ^{95}Zr and ^{97}Zr nuclei do not have unique spin-parity assignments (see Fig. 11). This calls for a new experimental effort in determining such basic properties before further progress in understanding the structure of these nuclei can be achieved. This is needed to trace, in spherical isotopes, the emergence of collectivity and deformation, which appear in heavier Zr isotopes.

ACKNOWLEDGMENTS

The authors thank Dr. Torsten Soldner and the technical services of the ILL and GANIL for supporting the EXILL campaign.

[1] K. Heyde and J. L. Wood, Rev. Mod. Phys. **83**, 1467 (2011).
[2] T. Werner, J. Dobaczewski, M. W. Guidry, W. Nazarewicz, and J. A. Sheikh, Nucl. Phys. A **578**, 1 (1994).
[3] J. Skalski, S. Mizutori, and W. Nazarewicz, Nucl. Phys. A **617**, 282 (1997).
[4] W. Urban, J. L. Durell, A. G. Smith, W. R. Phillips, M. A. Jones, B. J. Varley, T. Rząca-Urban, I. Ahmad, L. R. Morss, M. Bentaleb, and N. Schultz, Nucl. Phys. A **689**, 605 (2001).
[5] W. Urban, J. A. Pinston, J. Genevey, T. Rząca-Urban, A. Złomaniec, G. Simpson, J. L. Durell, W. R. Phillips, A. G. Smith, B. J. Varley, I. Ahmad, and N. Schulz, Eur. Phys. J. A **22**, 241 (2004).
[6] T. Rząca-Urban, W. Urban, M. Czerwiński, J. Wiśniewski, A. Blanc, H. Faust, M. Jentschel, P. Mutti, U. Köster, T. Soldner, G. de France, G. S. Simpson and C. A. Ur, Phys. Rev. C **98**, 064315 (2018).
[7] K. Sonnabend, A. Mengoni, P. Mohr, T. Rauscher, K. Vogt, and A. Zilges, Nucl. Phys. A **719**, C123 (2003).
[8] K. Sonnabend, P. Mohr, A. Zilges, R. Hertenberger, H.-F. Wirth, G. Graw, and T. Faestermann, Phys. Rev. C **68**, 048802 (2003).
[9] M. Guttormsen, S. Goriely, A. C. Larsen, A. Görgen, T. W. Hagen, T. Renstrøm, S. Siem, N. U. H. Syed, G. Tagliente, H. K. Toft, H. Utsunomiya, A. V. Voinov, and K. Wikan, Phys. Rev. C **96**, 024313 (2017).
[10] H. Niizeki and T. Tamura, J. Phys. Soc. Jpn. **52**, 3743 (1983).
[11] P. Cavallini, E. Monnamd, and A. Moussa, J. Phys. France **34**, 675 (1973).
[12] C. R. Bingham and G. T. Fabin, Phys. Rev. C **7**, 1509 (1973).
[13] S. K. Basu, G. Mukherjee, and A. A. Sonzogni, Nucl. Data Sheets **111**, 2555 (2010).
[14] I. F. Barchuk, G. V. Belykh, V. I. Golyshkin, A. F. Ogorodnik, and M. M. Tuchinskii, Izv. Akad. Nauk SSSR, Ser. Fiz. **41**, 101 (1977) [Bull. Acad. Sci. USSR, Phys. Ser. **41**, 82 (1977)].
[15] M.-G. Porquet *et al.*, Acta Phys. Pol. B **27**, 179 (1996).
[16] N. Fotiades, J. A. Cizewski, J. A. Becker, L. A. Bernstein, D. P. McNabb, W. Younes, R. M. Clark, P. Fallon, I. Y. Lee, A. O. Macchiavelli, A. Holt, and M. Hjorth-Jensen, Phys. Rev. C **65**, 044303 (2002).
[17] D. Pantelica, I. G. Stefan, N. Nica, M.G. Porquet, G. Duchene, A. Astier, S. Courtin, I. Deloncle, F. Hoellinger, A. Bauchet, N. Buforn, L. Donadille, O. Dorvaux, J. Duprat, B.J.P. Gall, C. Gautherin, T. Kutsarova, S. Lalkovski, R. Lucas, M. Meyer, A. Minkova, A. Prevost, N. Redon, N. Schulz, H. Sergolle, O. Stezowski, T. Venkova, and A. Wilson, Phys. Rev. C **72**, 024304 (2005).
[18] E. Moll, H. Schrader, G. Siegert, H. Hammers, M. Asghar, J. P. Bouget, P. Armbruster, H. Ewald, and H. Wollnik, Kerntechnik und Atompraxis **19**, 374 (1977).
[19] M. Jentschel, A. Blanc, G. de France, U. Koster, S. Leoni, P. Mutti, G. Simpson, T. Soldner, C. Ur, W. Urban *et al.*, J. Instrum. **12**, P11003 (2017).
[20] A. Złomaniec, H. Faust, J. Genevey, J. A. Pinston, T. Rząca-Urban, G. S. Simpson, I. Tsekhanovich, and W. Urban, Phys. Rev. C **72**, 067302 (2005).
[21] W. Urban, J. A. Pinston, G. S. Simpson, A. G. Smith, J. F. Smith, T. Rząca-Urban, and I. Ahmad, Phys. Rev. C **80**, 037301 (2009).
[22] D. Kameda, T. Kubo, T. Ohnishi, K. Kusaka, A. Yoshida, K. Yoshida, M. Ohtake, N. Fukuda, H. Takeda, K. Tanaka, N. Inabe, Y. Yanagisawa, Y. Gono, H. Watanabe, H. Otsu *et al.*, Phys. Rev. C **86**, 054319 (2012).
[23] W. Urban, K. Sieja, T. Rząca-Urban, J. Wiśniewski, A. Blanc, M. Jentschel, P. Mutti, U. Köster, T. Soldner, G. de France, G. S. Simpson, C. A. Ur, A. G. Smith, and J. P. Greene, Phys. Rev. C **104**, 064309 (2021).

[24] W. Urban, M. Jentschel, B. Märkisch, Th. Materna, Ch. Bernards, C. Drescher, Ch. Fransen, J. Jolie, U. Köster, P. Mutti, T. Rząca-Urban, and G. S. Simpson, J. Instrum. **8**, P03014 (2013).
[25] M. Wang *et al.* Chin. Phys. C **45**, 030003 (2021).
[26] R. Rodriguez-Guzman, P. Sarriguren, and L. M. Robledo, Phys. Rev. C **82**, 044318 (2010).
[27] J. F. Sharpey-Schafer, S. M. Mulins, R. A. Bark, J. Kau, F. Komati, E. A. Lawrie, J. J. Lawrie, T. E. Madiba, P. Maine, A. Minkova, S. H. T. Murray, N. J. Ncapayi, and P. A. Vymers, Eur. Phys. J. A **47**, 5 (2011).
[28] J. F. Sharpey-Schafer, R. A. Bark, S. P. Bvumbi, T. R. S. Dinoko, and S. N. T. Majola, Eur. Phys. J. A **55**, 15 (2019).
[29] N. Nica, Nucl. Data Sheets **111**, 525 (2010).
[30] D. K. Sharp, B. P. Kay, J. S. Thomas, S. J. Freeman, J. P. Schiffer, B. B. Back, S. Bedoor, T. Bloxham, J. A. Clark, C. M. Deibel *et al.*, Phys. Rev. C **87**, 014312 (2013).
[31] E. T. Gregor, M. Scheck, R. Chapman, L. P. Gaffney, J. Keatings, K. R. Mashtakov, D. O'Donnell, J. F. Smith, P. Spagnoletti, M. Thürauf, V. Werner, and C. Wiesman, Eur. Phys. J. A **53**, 50 (2017).
[32] K. Nomura, L. Lotina, T. Nikšić, and D. Vretenar, Phys. Rev. C **103**, 054301 (2021).
[33] Ł. W. Iskra, R. Broda, R. V. F. Janssens, M. P. Carpenter, B. Fornal, T. Lauritsen, T. Otsuka, T. Togashi, Y. Tsunoda, W. B. Walters, and S. Zhu, Phys. Lett. B **788**, 396 (2019).
[34] E. T. Gregor, N. N. Arsenyev, M. Scheck, T. M. Shneidman, M. Thurauf, C. Bernards, A. Blanc, R. Chapman, F. Drouet, A. A. Dzhioev *et al.*, J. Phys. G: Nucl. Part. Phys. **46**, 075101 (2019).
[35] G. Lhersonneau, P. Dendooven, S. Hankonen, A. Hankonen, M. Huhta, R. Julin, S. Juutinen, M. Onionen, H. Penttilä, A. Savelius, S. Törmänen, J. Äystö, P. A. Butler, J. F. C. Cocks, P. M. Jones, and J. F. Smith, Phys. Rev. C **54**, 1117 (1996).
[36] D. Abriola and A. A. Sonzogni, Nucl. Data Sheets **107**, 2423 (2006).
[37] W. B. Walters, Nucl. Phys. A **688**, 318 (2001).
[38] W. Urban, U. Köster, M. Jentschel, P. Mutti, B. Märkisch, T. Rząca-Urban, Ch. Bernards, Ch. Fransen, J. Jolie, T. Thomas, and G. S. Simpson, Phys. Rev. C **94**, 011302(R) (2016).